Effect of shoulder cavity and welding parameters on friction stir welding of thin copper sheets

R. M. Leal[1,2], N. Sakharova[1], P. Vilaça[3], D. M. Rodrigues[1] and A. Loureiro*[1]

The aim of this investigation was to study the influence of shoulder cavity and welding parameters on torque, defect formation, microstructure and mechanical properties of friction stir welds in very thin sheets of deoxidised copper. Three types of tools were used: a flat shoulder tool and two tools with conical shoulder cavities of 3 and 6° respectively. The welding parameters analysed were tool rotation and traverse speeds. It was observed that the torque, the microstructure and hardness and the formation of defects in the welds are influenced mainly by tool rotation speed and, to a lesser extent, by the traverse speed and shoulder cavity. The tensile properties of welds carried out at high rotation speeds are little affected by the shoulder cavity.

Keywords: FSW, Tool shoulder cavity, Copper alloys, Thin sheets

Introduction

Friction stir welding welding (FSW) is a solid state process developed by The Welding Institute, in the 1990s, for joining soft materials, such as aluminium alloys. In recent years, most of the research in FSW has been concentrated on the study of the effect of the principal process parameters (tool geometry, tool rotation and traverse speed, tool plunge force and tool tilt angle) on the quality of aluminium welds, mainly in terms of defect formation and metallurgical and mechanical properties.[1,2] Although it has been recognised that the tool geometry is crucial to regulate material flow during the process, the effect of the different tool features on the material flow is not still understood due to the variety and complexity of the developed geometries.[3,4] Moreover, in recent years, several studies have addressed the effect of the main welding parameters on heat generation during the process.[5,6] Finally, most of the studies mentioned above concentrate on the joining of thicknesses above 4 mm, and very few are focused on thicknesses of 1 mm or under, where more precise control of the process parameters is required.[7,8]

An important research effort is currently being undertaken to enable this welding technique to join harder materials, such as steels, titanium, magnesium and copper alloys and metal matrix composites.[9,10] Among those, the copper alloys show promise for applications in equipment requiring welding, such as heat exchangers, coolers, canisters for nuclear waste, etc. However, these alloys are difficult to join by fusion welding processes due to their high thermal conductivity and their susceptibility to solidification cracking and blowhole formation.[11] Although FSW seems to fulfil the requirements for overcoming the weld cracking problems because joining occurs in the solid state, very few studies concerning its application for welding copper alloys are available. Indeed, most of them concentrate on the welding parameters and on the microstructure and mechanical properties of welds in thick plates.[12,13] Significant reductions in hardness have been reported in FSW welds of commercial pure copper.[12,13]

Although the selection of adequate tool materials for joining copper has already been addressed,[13] the effect of tool cavity on the welding process has not yet been analysed in detail. The aim of the current study was to investigate the effect of shoulder cavity and welding parameters on defect formation, microstructure and mechanical properties of welds in very thin copper sheets.

Experimental

Phosphorus deoxidised copper sheets temper class R240, 1 mm thick and 250 mm long, were butt friction stir welded using an ESAB Legio FSW 3U machine. Three different tools, composed of 13 mm diameter shoulders and right threaded cylindrical probes 3 mm in diameter and 0·9 mm long, made of quenched and tempered H13steel, were used to produce the welds. A 13 mm shoulder diameter was selected in order to show the contribution of the shoulder to the weld process. The pin diameter and length were selected from previous tests in order to guarantee adequate tool strength and sound welds. The shoulder surface of one tool was flat, and the two other tools contained conical cavities of 3 and 6° respectively. All the welds were carried out using plunge

[1]CEMUC, Department of Mechanical Engineering, University of Coimbra, Portugal
[2]ESAD.CR, Polytechnic Institute of Leiria, Caldas da Rainha, Portugal
[3]DEM-IST, Technical University of Lisbon, Portugal

*Corresponding author, email altino.loureiro@dem.uc.pt

Published by Maney on behalf of the Institute
Received 5 July 2010; accepted 25 September 2010
DOI 10.1179/1362171810Y.0000000005

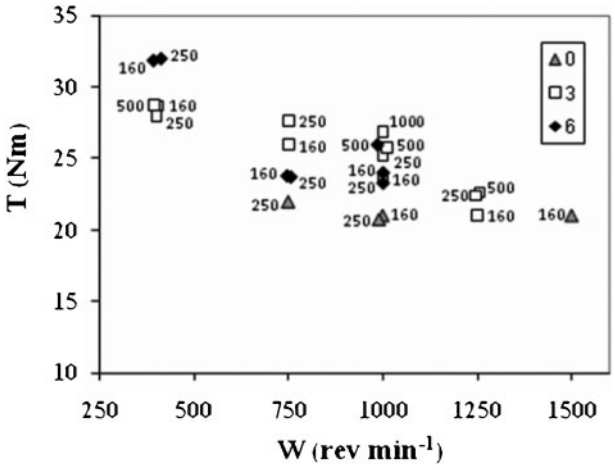

1 Torque versus rotational speed: data labels show weld traverse speed

force control. Several preliminary FSW experiments were performed in order to determine suitable values for plunging force, tool rotation and traverse speeds. In the tests presented in this article, the tool plunge force and the tilt angle were kept constant (7000 N and 2° respectively), while the tool rotation speed was set to 750 or 1000 rev min^{-1} and the traverse speed to 160 or 250 mm min^{-1}. Higher and lower rotational and traverse speeds than those mentioned were also tested, but most of them led to defective welds. The main welding conditions considered in this paper and the corresponding weld identifications are summarised in Table 1. Hereafter, the samples removed from the different weld series will be identified using a sequence of characters of the type *XWYVZ*, in which *X* corresponds to the shoulder cavity angle, *Y* represents the rotation speed of the tool (10 for 1000 rev min^{-1} and 7 for 750 rev min^{-1}) and, finally, *Z* represents the traverse speed of the tool (16 for 160 mm min^{-1} and 25 for 250 mm min^{-1}). In this way, the notation 0W10V16 identifies a weld carried out with the flat shoulder tool (0°) at 1000 rev min^{-1} and 160 mm min^{-1} of traverse speed.

Macroscopic examination of the welds was performed before the metallographic analysis, in order to detect surface defects. Metallographic specimens were removed transverse to the welding direction, polished and etched by immersion for 20 s in a solution consisting of $FeCl_3$ (2·5 g), H_2O (100 mL) and HCl (15 mL), at room temperature. The grain size of the base material and welds was measured using the mean linear intercept method. Specimens (TEM) were prepared by conventional procedures. Vickers hardness was measured using a 200 gf load for 15 s. Root bending and tensile testing were carried out on transverse specimens.

Table 1 Process parameters and defects detection*

Shoulder cavity angle, °	Reference	ω, rev min^{-1}	v, mm min^{-1}	Defect
0	0W7V16		160	IRP
	0W7V25	750	250	IRP
	0W10V16		160	IRP
	0W10V25	1000	250	IRP
3	3W7V16		160	IRP
	3W7V25	750	250	IRP
	3W10V16		160	…
	3W1025	1000	250	…
6	6W7V16		160	KB
	6W7V25	750	250	KB+V
	6W10V16		160	…
	6W10V25	1000	250	…

*IRP: incomplete root penetration; KB: kissing bond; V: voids.

Results and discussion

Weld torque

The torque, registered by the monitoring system during FSW, can provide a general idea of the readiness of the material to flow around the tool and about the power required in the process, which is influenced by material properties, welding parameters and tool geometry. Figure 1 illustrates the influence of the welding parameters and tool geometry on measured torque for welds carried out with the welding parameters indicated in Table 1. In the figure, some results of welds carried out at 400, 1250 and 1500 rev min^{-1} and 500 and 1000 mm min^{-1} traverse speed are also presented, in order to better illustrate the effect of these parameters on the torque. The data labels in the image indicate the traverse speed of each weld. As can be seen in the image, the torque decreases with increasing rotational speed for all tool geometries used. This decrease in the measured torque can be related to the decrease in the material flow stress at higher temperatures, associated with higher rotational speed. Although the weld temperature was not measured in the present investigation, the effect of the rotational speed on the heat generation rate and temperature has already been analysed by several authors that reported increasing peak temperatures with increasing tool rotation rates.[2,14,15] Similar evolution of the torque with rotation rate has already been observed for welds in aluminium alloys.[16,17]

The traverse speed also plays an important role in the required torque and quality of the welds. For the same tool and rotation rate, the highest torques in the graph correspond to the highest traverse speeds; for example, for welds carried out with the 3° conical cavity and 1000 rev min^{-1}, the two highest torque values in the image correspond to traverse velocities of 1000 and 500 mm min^{-1}, while the lowest torques correspond to speeds of 250 and 160 mm min^{-1} respectively. The increase in feed rate reduces the energy per unit of length of the weld, as mentioned by Khandkar *et al.*,[18] leading to a higher torque required for plastic deformation. The effect of traverse speed on torque tends to decrease for low and high rotation rates, as illustrated in the image for the 3° shoulder tool at 400 and 1250 rev min^{-1}. These results seem to contradict the computed values of Arora *et al.*,[19] which mentioned that the torque is relatively insensitive to the traverse speed. One explanation for that can be the little rotational speed (300 rev min^{-1}) used by those authors in the comparative study.

The image also shows that in the welds carried out with conical shoulder cavities of 3 and 6°, torque develops differently with respect to the rotation rate. For a rotational speed of 400 rev min^{-1}, the 6° shoulder tool requires higher torque than the 3° tool, while for 1000 rev min^{-1}, the required torque is similar for both tools. This suggests differences in the material flow and heat generated in the thermomechanically affected zone

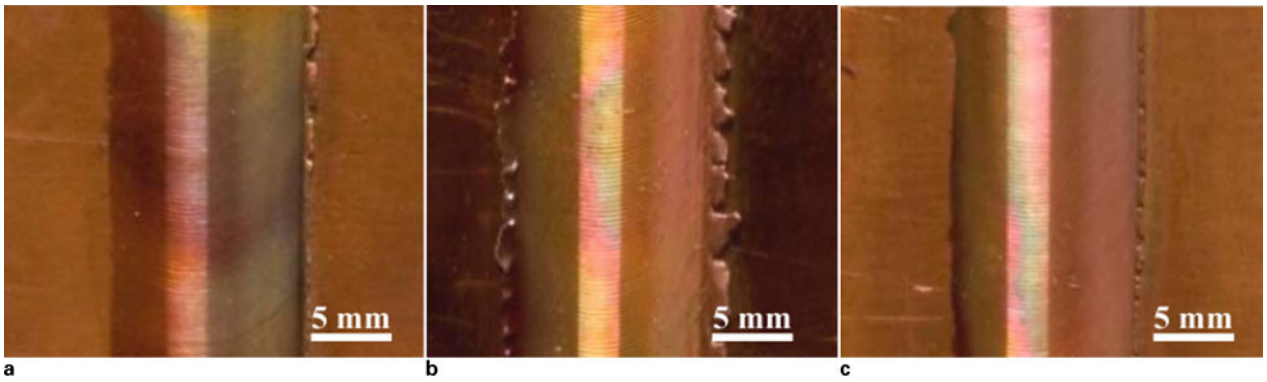

2 Appearance of *a* 0W10V25, *b* 3W10V25 and *c* 6W10V25 weld crowns

(TMAZ) of welds carried out with both tools. The torque measured in welds carried out with the flat shoulder shows similar development with rotation speed, but with lower values than those measured in welds carried out with the other tools, for all speeds tested. This torque reduction cannot be attributed to an increase in heat generated because the hardness and grain size in the nugget are identical to that observed in other welds, as shown below, but presumably to the decrease in volume of material swept by the tool. The volume of material deformed by the tool is difficult to distinguish in the cross-section, especially for welds carried out with high rotational speeds; however, the welds carried out with the flat shoulder showed a significant lack of root penetration, as indicated in Table 1 and discussed below. According to Cui *et al.*,[20] torque is primarily determined by the shoulder flow volume per revolution. However, as the tool rotation speed increases, the torque required by the different tools tends to be similar, showing a value ~21 N m in the case under study. In summary, the torque required for welding is also influenced by the tool shoulder cavity, although this influence tends to decrease with increasing tool rotation rate.

Weld morphology

Pictures of the crowns of the 0W10V25, 3W10V25 and 6W10V25 welds, produced with different tools and similar welding parameters, are illustrated in Fig. 2. As can be seen in the image, the weld crowns appear very smooth, with very fine regularly distributed arc shaped striations, independent of tool geometry. A small intermittent flash was observed on both sides of the welds. This flash is much more apparent in welds carried out with the 3° conical cavity than in welds carried out with other shoulder geometries, showing that the material flow under the shoulder is influenced by the angle of the shoulder cavity. Schmidt *et al.*[21] mentioned that the purpose of the shoulder cavity is to act as an escape volume for the material displaced by the pin, thereby enhancing the extrusion and consolidation of the material during welding. On the other hand, the

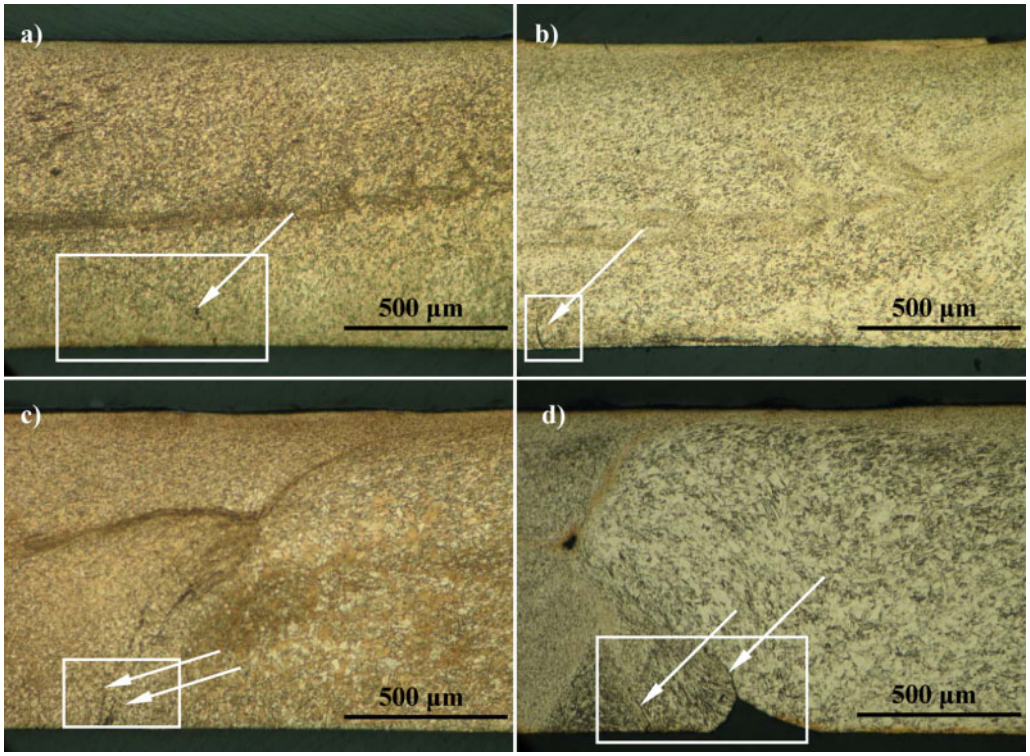

3 Defects in TMAZ of welds
a 0W7V16 (centre); *b* 3W7V25 (centre); *c* 6W7V16 (advancing side); *d* 6W7V25 (advancing side)

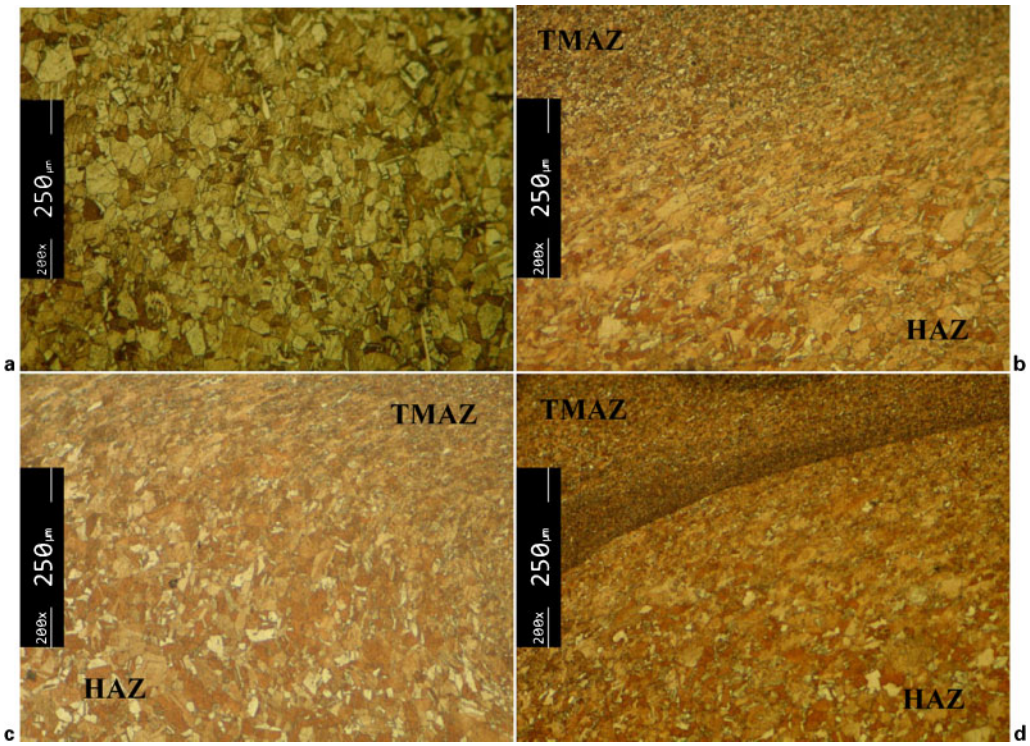

4 Microstructures of *a* base material and at transition between the TMAZ and HAZ, *b* at advancing side of weld 6W10V25 and *c* at retreating and *d* advancing sides of weld 3W7V25

authors have demonstrated in a previous publication[8] that shoulder promotes the transport of material at the top surface, from the retreating to the advancing side, and pushes it downward within the pin diameter. In this case, the 3° conical cavity is not sufficient to do that job, allowing material to escape as flash. The small flash for 6° shoulder cavity welds suggests that the volume under the shoulder is sufficient to constrain the material displaced by the pin and shoulder. By his side, the 0° shoulder seems to have little capacity to drag material, dragging mainly the material displaced by the pin and does not produce flash. It was also found that the tool geometry and welding parameters had little effect on weld width and thinning. A thinning between 3 and 7% was observed in the welds, although it was more apparent for welds carried out with the 3° conical cavity than for the others. This is consistent with the larger amount of flash seen in these welds.

Despite the weld crowns' very good appearance, visual inspection, root bending tests and metallographic analysis

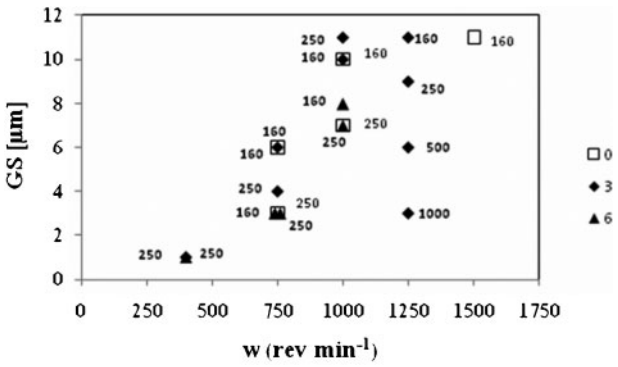

5 Effect of rotational speed on nugget grain size (GS): data labels show weld traverse speed

revealed the existence of root defects (RDs) in all welds carried out with flat shoulder and welds carried out with conical shoulders at 750 rev min^{-1}. Table 1 summarises this analysis. According to the table, only the welds carried out with conical shoulder tools at 1000 rev min^{-1} were free of RDs. Since welds carried out with lower rotation rates (down to 400 rev min^{-1}) also displayed RDs, 1000 rev min^{-1} can be considered the lower boundary of the process window for that tool design.

Figure 3 shows the TMAZ of welds carried out with different tools. As can be seen, the morphology of the RDs changes according to tool geometry. For the welds carried out with the flat shoulder, as shown in Fig. 3*a* for a weld 0W7V16, the RD consists of a long sharp discontinuity extending towards the retreating side of the weld. For the 3W7 welds, as illustrated in Fig. 3*b* for 3W7V25, the discontinuity is very small and is hard to detect by visual inspection. A detailed analysis of the root of the welds carried out with both tools showed that the morphology and size of the discontinuity is less affected by the traverse speed and is positioned in the initial interface between the faying surfaces of the plates. The material flow path and the curvature of the discontinuities illustrated in the images show that the plastic deformation at the root was insufficient to establish the coalescence of the plates. These results suggest that, for the plunge force applied, the tool shoulder geometry and rotation rate used did not generate enough heat to ensure proper plasticisation of the base material, leaving the end of the pin too far from the anvil. For the 6W7V16 welds (Fig. 3*c*), the RD is composed of two small cracks aligned with the oxide arrays extending through the weld thickness and located in the advancing side near the path of the pin. In this case, the defect can be related to the deposition of brittle oxides at the weld root and is known as a kissing bond. Sato *et al.*[15] suggested that these oxide

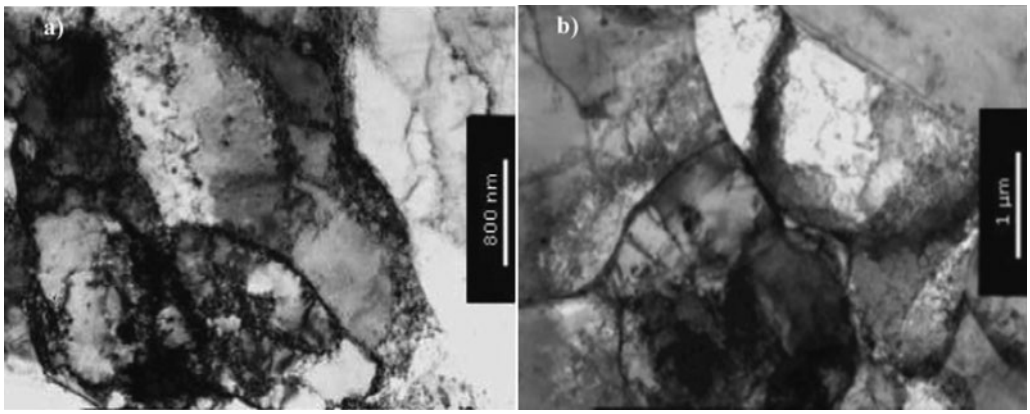

6 Images (TEM) from nugget of welds *a* 0W10V25 and *b* 3W10V25

deposits derive from the initial oxide layer on the plate surface, which is fragmented during the FSW process and distributed as oxide particles in a line in the cross-section. Several authors mention that kissing bond formation is influenced by material flow around the tool.[22,23] This is clearly visible from the 6W7V25 weld, for which the defect is composed of a wake of missing material, which had to be dragged by the tool from the weld root, and two very thin cracks, parallel to each other. One of the cracks is located at the end of the wake and the other at its left side at the interface of two different material structures. In this weld, it is also possible to see a very small hole in the mid-plate thickness. This figure suggests that the flow of material in the periphery of the pin tool is inadequate. The authors have shown in a previous work on welds in 1 mm thick aluminium sheets that part of the material drawn by the shoulder to the shear layer is pushed down around the pin towards the root of the weld.[8] Since the 6W10 welds performed at 1000 rev min^{-1} were free of defects, it is possible to conclude that the lower heat input associated with the lower rotation speed prevented adequate material flow close to the root of the weld, where there is also a significant extraction of heat via the backing plate, as mentioned by Rosales *et al.*[24] The increase in the pin length from 0·9 to 1 mm can reduce RDs for welds carried out at 750 rev min^{-1}, but the pin tip touches the anvil at 1000 rev min^{-1}.

By comparing the morphology of all the welds, it is evident that material flow is influenced by the conjugated effects of shoulder geometry and welding parameters. The use of the flat shoulder failed to produce welds free of defects, even for the highest rotation rate, due to the inability of the shoulder to drag sufficient material to the shear layer and push it downwards within the pin diameter.

Microstructural analysis

The microstructure of the base material, which is shown in Fig. 4*a*, is characterised by approximately equiaxial grains with an average grain size of 18 μm, with dark oxide particles dispersed inside and annealing twins extending across many grains. In contrast, all the welds had very refined grains in the TMAZ, as shown in Fig. 4*b–d* for 6W10V25 and 3W7V25 welds, in the transition between the TMAZ and heat affected zone (HAZ). This refinement is generally attributed to the occurrence of dynamic recrystallisation during the weld process.[25] Grain size measurements in the nugget of the welds indicate that it ranges from 1 to 11 μm, increasing with increasing tool rotation speed and decreasing traverse speed, as is shown in Fig. 5. The data labels shown in the image correspond to traverse speed used in each test. Xie *et al.*[25] found an increase in the grain size in the nugget for increasing rotation speeds in thicker plates of pure copper. The authors' results are in strong agreement with the values of torque registered for each weld in Fig. 1. For low rotation rate, torque is high, suggesting low heat generated and small grain size, as opposed to high rotation rate. High traverse speed requires high torque and produces little grain size, too, as little as the traverse speed increases. Shoulder cavity has little effect on grain size, although the grain size is not uniform inside the nugget, especially for welds carried out with the 6° cavity, where for weld 6W10V16,

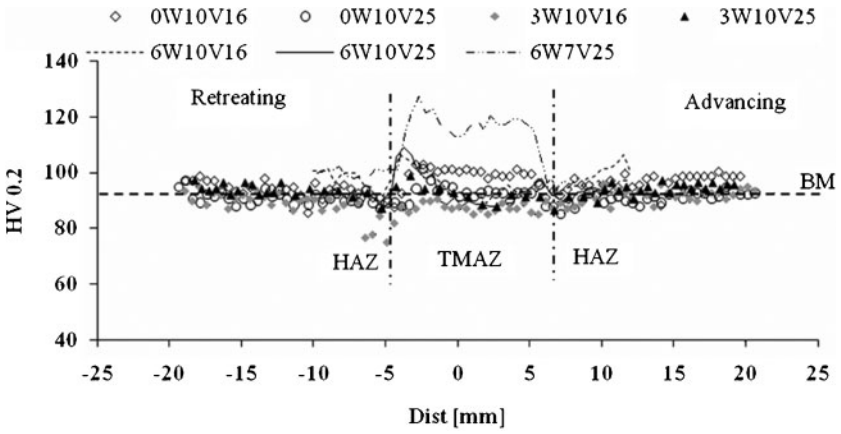

7 Hardness profiles, transverse to welding direction, measured at top surface of W10 and 6W7V25 welds

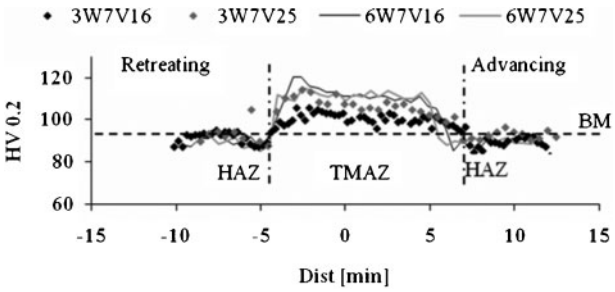

8 Hardness profiles for conical shoulders W7 welds

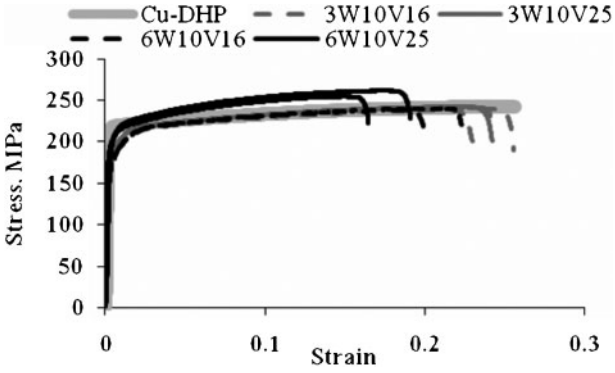

9 Tensile stress–strain curves for base material and non-defective welded samples

the grain size was 6 μm close to the retreating side in contrast to 8 μm at the centre.

The shoulder geometry affects mainly the shape of the TMAZ. In fact, the welds carried out with the flat or the 6° conical shoulder tools have more abrupt transitions between the TMAZ and the HAZ on the advancing side of the welds, displaying a narrow zone of plastically deformed but not recrystallised grains. This transition is as abrupt as the tool rotation speed is low and the traverse speed high, as illustrated in Fig. 3*c* and *d* for the 6W7V16 and 6W7V25 welds respectively. For the rotational speed of 1000 rev min^{-1}, the abrupt transition in the advancing side is less obvious, as shown in Fig. 4*b*. The welds have less evident TMAZ/HAZ transitions on the retreating side than on the advancing side, as shown in Fig. 4*c* and *d* for welds carried out with 3° conical shoulder.

Figure 6 displays examples of TEM images of the nugget of the 0W10V25 and 3W10V25 welds respectively. The images show that the microstructure is similar in both welds and is composed of fine recrystallised grains, which exhibit some elongation, presumably in the direction of main plastic deformation, and dislocation tangles and cells inside the grains. However, these cell structures are not well organised and the cell walls are poorly developed, which indicates that the density of dislocations is relatively low. Some interior grain areas are almost free from dislocations. This morphology suggests incomplete recrystallisation or modest plastic deformation on dynamic recrystallisation. Current results indicate that tool geometry has little effect on the micromechanisms of plastic deformation occurring in the welds performed at 1000 rev min^{-1}.

In conclusion, the microstructure of TMAZ is mainly influenced by the rotation and traverse speeds of the tool, although the shoulder cavity also has an important role in the morphology of that area.

Hardness

The microhardness profiles, measured transverse to the welding direction, for all the welds carried out at 1000 rev min^{-1}, together with the hardness profile for the 6W7V25 weld, are shown in Fig. 7. The average hardness of the base material is indicated in the same graph by a horizontal dotted line. The approximate location of the TMAZ is indicated by vertical dotted lines. These results show that the W10 welds only exhibit small changes in hardness through the TMAZ, irrespective of the geometry of the shoulder. This behaviour results from the competing effects of softening, caused by dynamic recrystallisation, and hardening resulting from the plastic strain or grain refinement in the stir zone. However, for the welds carried out with conical shoulder tools, some hardening was reported at the limits of the TMAZ, both on the advancing and retreating sides and chiefly in the 6° conical shoulder welds. This is probably due to greater plastic deformation induced by the external border of the shoulder. In fact, a more refined grain structure in this zone was detected in the metallographic analysis.

The effect of tool rotation speed on hardness can also be inferred from Fig. 7 by comparing the hardness profiles of welds 6W7V25 and 6W10V25. The former shows hardness results in the TMAZ well above the second. This behaviour is in good agreement with the torque measurement results (Fig. 1), which show that the lower rotational speed requires higher weld torque, suggesting that there is less heat generated during the process, and there are therefore lower recrystallisation rates, leading to harder welds.

This increase in hardness was observed for all the welds carried out at 750 rev min^{-1}, independent of tool geometry, as shown in Fig. 8 for the conical shoulder tools. The effect of rotational speed on hardness was even more evident in the preliminary welds performed with the same tools, but at 400 rev min^{-1}, where an average hardness of 145 HV0·2 was registered in the TMAZ, these welds were subject to severe RD. From Figs. 7 and 8, it is also possible to conclude that the effect of the tool traverse speed on the TMAZ's hardness is small. In fact, when tool traverse speed is considered, the most significant variation in hardness was between welds 3W7V25 and 3W7V16, but it did not exceed 8%.

Therefore, in conclusion, it is possible to say that the distribution of hardness in the TMAZ of friction stir welds in that range is mainly influenced by tool rotation speed and in lower extent by the traverse speed and tool geometry.

Table 2 Results of transverse tensile tests*

Reference	Tensile strength, MPa	Elongation at maximum load, %	Weld efficiency
Cu-DHP	249	26	…
3W10V16	239	22·5	0·96
3W10V25	242	23	0·97
6W10V16	239	20	0·96
6W10V25	257	16·5	1·0

*Cu-DHP: phosphorus deoxidised copper sheets.

Tensile properties

The nominal tensile stress–strain curves for the base material and transverse welded samples, free of defects, are shown in Fig. 9. Each weld series is illustrated by

a 3W10V25; *b* 6W10V16

10 Top view of fractured tensile specimens

two plots using open and closed symbols with the same mould. By analysing the figure, it is possible to conclude that the base material underwent a small amount of hardening during plastic deformation and displayed very good plasticity, reaching at least 26% strain on fracture. The welded samples display only small changes in yield and tensile strengths relative to the base material and some reduction in the elongation at maximum load. Table 2 summarises the average results obtained for stress and strain at maximum load as well the weld efficiency. The weld efficiency is defined as the rate of the tensile strengths of the weld to the base material. From Fig. 9 and Table 2, it is possible to conclude that the 6W10V25 welds are in tensile strength evenmatch relative to the base material, and all other welds are slightly in undermatch condition.

The analysis of the specimens after tensile testing revealed that the specimens removed from 3W10 welds failed in the TMAZ, as illustrated in Fig. 10*a*. As no significant softening was observed in these welds, the fracture in the TMAZ was certainly influenced by stress concentration resulting from the slight thinning in this zone. On the other hand, the 6W10 tensile specimens failed in the TMAZ or in the TMAZ/HAZ transition (*see* Fig. 10*b*), in the region where a sudden transition in hardness was observed, as shown in Fig. 7. Stronger welds are achieved using lower rotation rates, as suggested by the hardness values; however, these welding parameters do not produce welds free of defects.

Conclusions

The results and discussion presented above enable the following conclusions to be drawn.

1. Welds carried out using tools with conical cavity shoulders require spindle torques higher than those performed with flat shoulder tools; however, a more substantial increase in weld torque was observed with the reduction in tool rotation speed, for the same tool geometry.

2. The microstructure and hardness and the formation of defects in the welds are influenced mainly by the tool rotation speed and to a lesser extent by the traverse speed and shoulder cavity.

3. The tensile properties of welds carried out with conical shoulders and high rotational speed are little affected by the angle of the conical cavity, as they are approximately in the evenmatch condition.

Acknowledgements

The authors are indebted to the Portuguese Foundation for the Science and Technology through COMPETE program from QREN and to FEDER for the financial support and to company Thyssen Portugal–Aços e Serviços Lda for providing materials and heat treatments for the tools designed and fabricated in the project.

References

1. J. H. Yan, M. A. Sutton and A. P. Reynolds: *Sci. Technol. Weld. Join.*, 2005, **10**, (6), 725–736.
2. R. Nandan, T. DebRoy and H. K. D. H. Bhadeshia: *Prog. Mater Sci.*, 2008, **53**, (6), 980–1023.
3. W. M. Thomas, K. I. Johnson and C. S. Wiesner: *Adv. Eng. Mater.*, 2003, **7**, (5), 485–490.
4. Y. H. Zhao, S. B. Lin, F. X. Qu and L. Wu: *Mater. Sci. Technol.*, 2006, **22**, (1), 45–50.
5. C. M. Chen and R. Kovacevic: *Int. J. Mach. Tools Manuf.*, 2003, **43**, (13), 1319–1326.
6. P. Su, A. Gerlich, T. H. North and G. J. Bendzsak: *Sci. Technol. Weld. Join.*, 2006, **11**, (2), 163–169.
7. A. Scialpi, M. de Giorgi, L. A. C. de Filippis, R. Nobile and F. W. Panella: *Mater. Design*, 2008, **29**, (5), 928–936.
8. R. M. Leal, C. Leitão, A. Loureiro, D. M. Rodrigues and P. Vilaça: *Mater. Sci. Eng. A*, 2008, **A498**, (1–2), 384–391.
9. H. Fujii, L. Cui, N. Tsuji, M. Maeda, K. Nakata and K. Nogi: *Mater. Sci. Eng. A*, 2006, **A429**, (1–2), 50–57.
10. Y. Zhang, Y. S. Sato, H. Kokawa, S. H. C. Park and S. Hirano: *Mater. Sci. Eng. A*, 2008, **A485**, (1–2), 448–455.
11. A. Durocher, D. Ayrault, C. Chagnot, M. Lipa and W. Saikaly: *J. Nucl. Mater.*, 2007, **367–370**, (Part 2), 1208–1212.
12. W.-B. Lee and S.-B. Jung: *Mater. Lett.*, 2004, **58**, (6), 1041–1046.
13. K. Savolainen, J. Mononen, T. Saukkonen, H. Hanninen and J. Koivula: Proc. 5th Int. Symp. on 'Friction stir welding', Metz, France, September 2004, TWI. Session 05B - Copper Alloys & Magnesium Alloys, paper 2.
14. W. Tang, X. Guo, J. C. McClure, L. E. Murr and A. C. Nunes: *J. Mater. Process. Manuf. Sci.*, 1998, **7**, (2), 163–172.
15. Y. S. Sato, M. Urata and H. Kokawa: *Metall. Mater. Trans. A*, 2002, **33A**, (3), 625–635.
16. – J. W. Pew, T. W. Nelson and C. D. Sorensen: *Sci. Technol. Weld. Join.*, 2007, **12**, (4), 341–347.
17. K. J. Colligan and R. S. Mishra: *Scr. Mater.*, 2008, **58**, 327–331.
18. M. Z. H. Khandkar, J. A. Khan and A. P. Reynolds: *Sci. Technol. Weld. Join.*, 2003, **8**, (3), 165–174.
19. A. Arora, R. Nandan, A. P. Reynolds and T. DebRoy: *Scr. Mater.*, 2009, **60**, 13–16.
20. S. Cui, Z. W. Chen and J. D. Robson: Proc. 8th Int. Symp. on 'Friction stir welding', Timmendorfer Strand, Germany, May 2010, TWI, Paper 6B-4.
21. H. Schmidt, J. Hattel and J. Wert: *Modell. Simul. Mater. Sci. Eng.*, 2004, **12**, 143–157.
22. Y. S. Sato, H. Takauchi, S. H. C. Park and H. Kokawa: *Mater. Sci. Eng. A*, 2005, **A405**, (1–2), 333–338.
23. Y. G. Kim, H. Fujii, T. Tsumura, T. Komazaki and K. Nakata: *Mater. Sci. Eng. A*, 2006, **A415**, (1–2), 250–254.
24. M. Rosales, N. G. Alcântara, J. Santos and R. Zettler: Materials Science Forum Vols. 636-637 (2010) pp 459–464.
25. G. M. Xie, Z. Y. Ma and L. Geng: *Scr. Mater.*, 2007, **57**, (2), 73–76.